Enhanced Scheduling Strategy for Wind Farm−Flexible Load Joint Operation System

Tianhui Meng and Jilai Yu

***Abstract*—The increasing penetration of wind power poses challenges to the power grid operation and scheduling. Yet, if the uncertainty of wind power can be economically and effectively managed on the source side, it can drive the power grids towards renewable-dominant future. In this paper, an enhanced scheduling strategy for wind farm−flexible load joint operation system (WF-FLJOS) is proposed. The proposed strategy is designed to manage the uncertainty of wind power on the generation side when integrated into a large-scale power grid. Moreover, it can contribute to saving energy costs on the load side. Compared with the current wind farm operation rules, more stringent assessment requirements are put forward for wind power output accuracy, and the internal organization framework of WF-FLJOS is designed. For potential power violations of wind farms and flexible loads, the violation penalty mechanisms are developed to regulate the behavior of the participants. The joint operation model of the WF-FLJOS is proposed and the submission and tracking approach of the generation schedule for the wind farm is investigated. Numerical results indicate that the proposed strategy can not only improve the ability of the wind farm to track the generation schedule, but also consider the benefits of both the farm side and the load side. Meanwhile, the proposed strategy effectively reduces the schedule adjustment pressure on the main grid caused by the rolling correction mode of the intraday schedule for wind farms.**

***Index Terms*—Wind farm, flexible load, joint operation system, multi-time scale, generation schedule.**

NOMENCLATURE

A. Indices and Sets

+, −	Superscripts for microgrid (MG) charging and discharging
c	Index of cases
i	Index of 5 min intervals in 24 hours, $i=0,1,\dots,287$
k, r	Indices of segment of stepped tariffs offered by wind farm to thermostatically controlled load (TCL) agent and MG
s, S	Index and set of scenarios
t	Index of time for 15 min intervals
t_1	Index of time for 1 min intervals within 5 min intervals
T	Set of time

B. Parameters

α, β	Positive and negative allowed deviation factors
τ_s	Probability of scenario s
$\lambda^{\text{dev,sup}}$, $\lambda^{\text{dev,ins}}$	Penalty factors for positive and negative deviations
$\lambda^{\text{pen,sup(}'\text{)}}$, $\lambda^{\text{pen,ins(}'\text{)}}$	Positive and negative penalty factors for wind-unrestricted and wind-restricted stages
Δt	Time interval of 15 min
ΔL^{mg}	Interval between adjacent segment points in contract with MG, $\Delta L_t^{\text{mg},+}=L_t^{\text{mg,max},+}/3$
c_t^{g}	Feed-in tariff of wind power
$c^{\text{mg},r}$	Wind power price for MG
$c^{\text{tcl},k}$	Wind power price for TCL agent
c^{wc}	Penalty factor for curtailed wind power
$L^{\text{mg,max}}$	The maximum adjustable capacity of MG
$L^{\text{tcl,min}}$, $L^{\text{tcl,max}}$	The minimum and maximum adjustable capacities of TCL agent
$L^{\text{tcl},k}$	Segmentation point determined in contract with TCL agent
$P^{\text{w,max}}$	The maximum installed capacity of wind farm
P^{wa}	Available wind power
$P^{\text{ws}'}$	Wind-restricted command from main grid

C. Variables

$\delta_{t_1}^{\text{sup}}$, $\delta_{t_1}^{\text{ins}}$	Binary variables indicating magnitude relationship of $P_{t_1}^{\text{wg}}$ and $P_{t_1,\text{id}}^{\text{ws}}$
α_{tcl}	Allowed bi-directional fluctuation rate of node where TCL is located in distribution network (DN)

Manuscript received: March 5, 2024; revised: June 27, 2024; accepted: November 14, 2024. Date of CrossCheck: November 14, 2024. Date of online publication: February 21, 2025.

This work was supported by National Natural Science Foundation of China (No. 51877049).

T. Meng and J. Yu (corresponding author) are with the School of Electrical Engineering and Automation, Harbin Institute of Technology, Harbin, China (e-mail: mtianhui9@163.com; yupwrs@hit.edu.cn).

DOI: 10.35833/MPCE.2024.000244

$C^{\text{wf,tcl}}$, $C^{\text{wf,mg}}$	Revenues of wind farm from selling electricity to TCL agent and MG
C^{tcl}	Cost of TCL agent
$C_t^{\text{wf,mg,+}}$, $C_t^{\text{wf,mg,-}}$	Revenues of wind farm from selling electricity to MG and reverse discharging cost of MG
C^{wc}	Penalty of curtailed wind power
C^{wd}	Revenue of wind farm from selling electricity to flexible loads
C^{wf}	Operation revenue of wind farm
C^{dev}	Deviation penalty cost
C^{pen}	Deviation penalty cost of intraday schedule from day-ahead schedule or wind-restricted curve
C^{wg}	Revenue of wind farm from selling electricity to main grid
$\Delta C^{\text{WF-FLJOS}}$	Incremental revenue of wind farm−flexible load joint operation system (WF-FLJOS)
u^{sup}, u^{ins}	Binary variables indicating whether intraday schedule deviates from allowed range of day-ahead schedule or wind-restricted command
v_t^{res}	Binary variable indicating whether t is at wind-restricted stage
P^{tcl,b_1}, P^{tcl,b_2}	Power that can be supplemented and reduced by DN
P^{wc}	Curtailed wind power
P^{wg}	Power delivered from wind farm to main grid
$P_{t_1,\text{id}}^{\text{ws}}$	Schedule wind power output at intraday stage at $t_1/\Delta t''$ min
P^{w2tcl}	Power supplied from wind farm to TCL agent
P^{w2mg}, P^{mg2w}	Bidirectional power between wind farm and MG
$P_{t_{rt}}^{\text{dev,sup}}$, $P_{t_{rt}}^{\text{dev,ins}}$	Positive and negative deviation power beyond allowed range in current and look-ahead intervals
t_0	Current interval
$W_{i\Delta t'}^{\text{dev}}$	Sum of violation power in the i^{th} 5 min interval

I. Introduction

THE integration of large-scale wind energy poses problems to modern power system operation due to its strong randomness and volatility [1]. Therefore, wind farms need to cooperate with other resources to enhance their controllability. Currently, energy storage devices are predominantly deployed on the farm side to support its operation [2], [3]. On the one hand, the current construction and maintenance costs of energy storage remain high. Moreover, the accuracy of forecasts exhibits significant variations among different wind farms. Requring wind farms to install energy storage at a fixed percentage of their capacity (typically 10%-20%) to cope with wind power uncertainty may impact farm-side revenues and diminish the attractiveness of wind power development. On the other hand, the demand side encompasses a significant number of loads with demand flexibility, which can be treated as valuable resources that can participate in the system regulation. Thus, it is necessary to explore an economically and technically feasible strategy for coordinating wind farms with flexible loads to mitigate the impact of wind power uncertainty from the farm side.

Traditional coordination among generation sources, power grid, and loads aims to minimize the total system costs [4], [5] or maximize the social welfare [6], [7]. Flexible loads respond to commands or compensation prices from the grid dispatch center and participate in the optimization by adjusting their power consumption. The main grid operator needs to organize various types of flexible loads with different generation and consumption behaviors, and cover the corresponding compensation or incentive costs. Therefore, the source-grid-load synergy mechanism inevitably poses certain technical and economic challenges to the main grid operator.

Compared with handling wind power uncertainty by the main grid, the local consumers can be organized to help reduce energy transmission losses and relieve congestion, thus providing them with better consumption prices. The energy management model proposed in [8] aims to maximize the social welfare of the microgrid (MG) system by considering renewable energy uncertainty and demand response. A community-integrated energy system (CIES) optimization model with the objective of minimizing the daily comprehensive cost and carbon emissions is established in [9]. The above studies are primarily oriented to the localized utilization of wind power in MGs or CIES. However, many wind farms have a capacity of more than 100 MW and are located far from load centers. Therefore, the need for transmission to the external grid should be considered.

The grid connection requirements for wind power state that wind farms will be penalized if their actual wind power output accuracy fails to meet the standards [10]. In countries such as Sweden or Finland, the cost of non-compliance is 2-3 €/MWh, while in Bulgaria, energy default rates of up to 10-24 €/MWh may be imposed [11]. Thus, the power imbalance reduces the revenue of wind power operator. Wind power producers can strategically purchase reserve capacity to offset part of their deviation penalties [12]. Moreover, wind farms can operate in synergy with power sources, such as hydropower plants, combined heat and power (CHP) plants, and concentrating solar power (CSP) plants to reduce deviations in power output to the main grid. In [11], wind energy producers submit bids in conjunction with the hydro resources, and the mismatch between predicted energy and supplied energy is compensated by the hydro producers. Furthermore, the optimal bidding and tracking strategies for wind farms and hydro units are presented in [13]. In [14], a joint operation strategy for wind farms and CHP plant is established to improve the revenue of both parties. With the increase of wind power generation, relying solely on the regulation of traditional generation sources or a trivial amount of battery energy storage systems seems insufficient to ensure the reliability of the power system.

Meanwhile, many efforts are devoted to exploring the potential of using flexible loads to reduce the deviation of wind power to the main grid. In [15] and [16], the charging and discharging capabilities of electric vehicles (EVs) are utilized to smooth the penalty costs arising from overestimations and underestimations of the available wind power. The aforementioned studies mainly focus on addressing the technical problems of the coordination between wind farm and load, while neglecting their economic needs. Given that wind farms and loads have different ownerships, the benefits of the participants on the load side should also be considered. Studies on the benefits of the participants on the load side can be primarily divided into three categories: ① setting compensation prices in the bilateral contract [17]; ② calculating benefits based on price settlements influenced by supply and demand relationships [18]; ③ allocating revenues based on the contribution of each participant on the load side [19], [20].

Photovoltaic (PV) energy is divided into forecast power and uncertain power in [18]. The uncertain power is balanced by flexible loads. The market mechanism is designed, and both PV owners and consumers can benefit from the peer-to-peer trading model. A coordinated bidding strategy for power-to-gas (P2G) facilities and wind energy producers is proposed in [19]. Under this strategy, wind farms provide electricity to the P2G and, in return, receive reserve capacity [19]. In [20], the wind farm and thermostatically controlled load (TCL) aggregators participate in cooperative bidding and trading strategies at the day-ahead stage and the regulation markets, where the asymmetric Nash bargaining is used to allocate the benefits. Allowing wind farms to adjust their schedule wind power outputs at the intraday stage can reduce the imbalance costs and the reserve capacity requirements in the real-time balancing market. In [21], a self-scheduling strategy for a virtual power plant (VPP) consisting of a wind farm, demand response, and energy storage is presented, enabling the VPP to participate at day-ahead stage, intraday stage, and balancing markets. Most of the aforementioned studies focus on the method of wind farms and flexible loads bidding together in the electricity market. However, the problem of violations in collaboration is ignored, and the specific cooperative business between the two entities is not clearly defined.

Motivated by the above-mentioned challenges, this paper proposes a collaborative operation framework that integrates the wind farm and flexible load. The main contributions of this paper are summarized as follows.

1) This paper proposes an enhanced scheduling strategy that utilizes flexible loads connected to wind farms through low-voltage distribution lines to absorb the uncertainties of wind power. Observed from the source side, the uncertainties of the wind power are thus reduced, and the propagation of the volatility to the upstream grid is accordingly reduced.

2) Based on the current wind farm operation rules, more stringent assessment requirements for wind power output accuracy are proposed. By leveraging the inherent adjustability of flexible loads and the balancing capacity provided by the distribution network (DN), the joint operation model of wind farm – flexible load joint operation system (WF-FLJOS) improves the schedule accuracy of wind power output.

3) Unlike the widely-used rolling correction mode, this paper allows the wind farm operator to make a single revision to the day-ahead schedule curve at the intraday stage. The aim is to relieve the pressure on the main grid operator from frequently revising the schedules.

4) Considering the uncertainty of load response and its collaborative relationship with the wind farm, the dispatch-feedback-response mechanism on the load side is designed. Additionally, penalties for load violations in the joint operation model are specified to clarify the responsibilities of each participant.

The rest of this paper is organized as follows. The architecture of WF-FLJOS is introduced in Section II. Section III illustrates the operation mechanism of WF-FLJOS. Section IV presents the joint operation model of WF-FLJOS. Case studies and conclusions are provided in Sections V and VI, respectively.

II. Architecture of WF-FLJOS

With the assessment requirements for wind power output accuracy becoming increasingly stringent, wind farms are confronted with three main challenges: ① how to improve the execution accuracy of grid integration schedule with limited forecast capability; ② how to ensure the operation revenues of the wind farms; and ③ how to reduce the regulatory burden on the grid caused by wind power output uncertainty. Moreover, when the uncertainty of wind power integrated into grid is substantial, the main grid has to rely on conventional units and other resources for regulation, which inevitably leads to higher energy costs for customers. To address these challenges, this study presents the WF-FLJOS.

The WF-FLJOS refers to the cooperative relationship established between the wind farm and nearby flexible loads that are connected via distribution lines. Through reasonable incentives and operation methods, WF-FLJOS can enhance the ability of wind farms to execute the schedule wind power output and improve the economic benefits for participants. Potential scenarios for the joint operation model include coastal wind farms with shoreside urban loads and suburban wind farms with nearby industrial parks. For instance, Jiangsu Province, China has released the plan of the new power system in coastal areas [22], which emphasises the need for dedicated transformers and distribution lines to promote local or nearby consumption of green power. The Inner Mongolia Autonomous Region is currently constructing integrated wind – solar – hydrogen projects [23], where the grid-connected projects are empowered to supply and purchase electricity from the main grid.

Figure 1 depicts the overall architecture of the WF-FLJOS. The participants include the flexible loads and wind farm, where the wind farm is the dominant participant. Flexible loads are categorized into two forms: highly controllable loads and load agents. Entities with high controllable capacity can directly engage in the WF-FLJOS, such as MGs and VPPs. The small- or medium-sized loads such as TCLs and EVs join the collaboration through load agents. The joint operation dispatch center (JODC) is the central component of the WF-FLJOS. JODC is responsible for collecting wind farm operation data, signing contracts with loads, delivering dispatch commands, and measuring load response results. As the leader of the WF-FLJOS, the wind farm can expand the capabilities of its existing control center to undertake the responsibilities of JODC. In the WF-FLJOS, flexible loads are connected to both the wind farm and the DN via smart switch devices. The smart switch devices can control the on/off state or the power ratio of the two distribution lines connecting the flexible load based on the commands from the JODC. Therefore, the proportion of power absorbed by the flexible load from the DN and the wind farm can be controlled in the joint operation model.

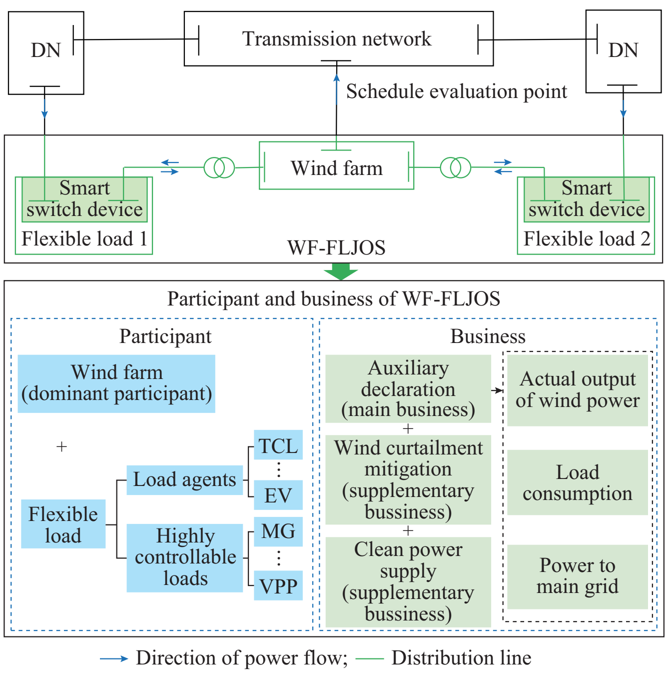

Fig. 1. Overall architecture of WF-FLJOS.

Various types of businesses can be developed in the WF-FLJOS, such as auxiliary declaration, wind curtailment mitigation, and clean power supply. Among them, auxiliary declaration serves as the main business, while the other two types of businesses are supplementary. The meanings of each type of business are as follows.

1) Auxiliary declaration business: the wind farm coordinates with flexible loads that are powered by two power sources and uses smart switch devices to manage the power distribution. The purpose of the auxiliary declaration business is to enhance the ability of the wind farm to declare and execute the schedule curve.

2) Wind curtailment mitigation business: the reverse-peaking characteristics of the wind power may result in wind curtailment when the regulation capacity is insufficient in main grid. Under such circumstances, wind producers can seek the assistance of flexible loads in WF-FLJOS to absorb this part of surplus energy, thereby increasing their operation revenues.

3) Clean power supply business: the wind farm can supply energy to electric cooling loads, electric heating loads, and hydrogen production loads via distribution lines, which facilitates the enhancement of the clean energy consumption on the load side.

In order to provide the WF-FLJOS with flexibility similar to that of the conventional units, the wind farm is required to collaborate with flexible loads and follow the schedule curve set by the main grid operator. When the actual wind power output exceeds the upper limit allowed by the main grid, the wind farm can increase the supply to flexible loads while reducing the wind power output to the main grid. When the actual wind power output falls below the lower limit allowed by the main grid, equivalent upward regulation capability can be obtained in two ways: ① by reducing the wind power supply to the flexible loads; and ② by increasing the output of load side distributed energy resources to reduce the demand for wind power from flexible loads or provide power directly to the wind farm-grid connection point. It is worth noting that transferring electricity directly from DN to the wind farm-grid connection point on load side is not permitted. Meanwhile, the power fluctuations in the DN connection lines should not exceed the permissible limits when the flexible loads are absorbing wind power.

III. OPERATION MECHANISM OF WF-FLJOS

The operation mechanisms of the WF-FLJOS are essential to its stable and efficient performance. Moreover, this section discusses the organization of the WF-FLJOS and the participation of flexible loads.

A. Main Grid Requirements for Wind Farm Schedule Curves

Current regulations require wind farms to submit the wind power forecast curves to the main grid operator at day-ahead and intraday stages. The accuracy of these forecast curves is evaluated through mean square deviation method [10]. However, when the wind penetration is high, the mean square deviation method may lead to inadequate regulation capacity and excessive regulation costs on the main grid. Therefore, considering the inherent uncertainty of wind power and the regulatory pressure on the grid, this study proposes three improvements to the main grid requirements for wind farm schedule curves and actual wind power output in grid connection rules. The three improvements are as follows.

1) In order to better meet the assessment requirements, wind farms are allowed to replace the wind power forecast curves with self-determined generation schedule curves at the day-ahead and intraday stages.

2) At the intraday stage, in order to alleviate the burden on the main grid caused by frequent rolling corrections to the schedule curves, wind farms are allowed to make only one correction to the schedule value, which must be implemented two hours before the operating period.

3) In order to assess the wind power output accuracy, a power generation curve evaluation method is adopted to re-

place the mean square deviation method [24].

The grid corporation calculates the actual deviation of wind power in 1 min interval ($\Delta t''=1$ min), and calculates the penalty costs for positive and negative violations in 5 min interval ($\Delta t'=5$ min). The sum of violation power is written as (1). In (1), $\delta_{t_1}^{\text{sup}}$ and $\delta_{t_1}^{\text{ins}}$ are the binary variables. If $P_{t_1}^{\text{wg}}-P_{t_1,\text{id}}^{\text{ws}}>0$, $\delta_{t_1}^{\text{sup}}=1$ and $\delta_{t_1}^{\text{ins}}=0$; and if $P_{t_1}^{\text{wg}}-P_{t_1,\text{id}}^{\text{ws}}\leq 0$, $\delta_{t_1}^{\text{sup}}=0$ and $\delta_{t_1}^{\text{ins}}=1$. It can be observed that the actual positive/negative violation power equals to the gap between the cumulative actual positive/negative deviation and the allowed deviation in 5 min. The resolution of the schedule curves submitted by the wind farm to the main grid is 15 min. Therefore, the schedule wind power output per minute is obtained through linear interpolation between adjacent points on the schedule curve.

$$W_{i\Delta t'}^{\text{dev}}=\Bigg[\max\Bigg(\sum_{t_1=i\Delta t'}^{i\Delta t'+4\Delta t''}|P_{t_1}^{\text{wg}}-P_{t_1,\text{id}}^{\text{ws}}|\delta_{t_1}^{\text{sup}}-\alpha_{\text{id/res}}\sum_{t_1=i\Delta t'}^{i\Delta t'+4\Delta t''}P_{t_1,\text{id}}^{\text{ws}},0\Bigg)+ \max\Bigg(\sum_{t_1=i\Delta t'}^{i\Delta t'+4\Delta t''}|P_{t_1,\text{id}}^{\text{ws}}-P_{t_1}^{\text{wg}}|\delta_{t_1}^{\text{ins}}-\beta_{\text{id/res}}\sum_{t_1=i\Delta t'}^{i\Delta t'+4\Delta t''}P_{t_1,\text{id}}^{\text{ws}},0\Bigg)\Bigg]\Delta t'' \tag{1}$$

$$P_{t_1,\text{id}}^{\text{ws}}=P_{t,\text{id}}^{\text{ws}}+\frac{t_1-t}{\Delta t''}\frac{P_{t+\Delta t,\text{id}}^{\text{ws}}-P_{t,\text{id}}^{\text{ws}}}{15} \tag{2}$$

where subscript id denotes intraday stage; and subscript res denotes wind-restricted stage.

B. Internal Organization of WF-FLJOS

1) Admission Rules for WF-FLJOS

In the WF-FLJOS, the wind farm serves as the dominant participant. The load side comprises numerous adjustable resources with different regulation capabilities. Therefore, the JODC should establish appropriate admission rules for WF-FLJOS, such as controllable capacity and response time. Additionally, flexible loads need to be configured with local control terminals or smart switch devices to respond to schedule commands or be directly controlled by the JODC. For example, TCLs can access smart home control terminals, where the electricity consumption behavior of users is analyzed and optimized by the load agents.

2) Internal Implement Process of WF-FLJOS

The internal implement process of the WF-FLJOS is as follows.

Step 1: JODC signs cooperation agreements with flexible loads that are willing to participate and meet the admission rules. These agreements include the business model, adjustable capacity range, and power supply price.

Step 2: at the day-ahead stage, JODC submits its schedule wind power output to the main grid based on the information, such as wind power forecast information and availability of flexible loads. Schedule corrections are then made at the intraday stage based on updated information.

Step 3: at the real-time stage, JODC selects and schedules specific loads or load agents based on ultra-short-term wind power forecast information to ensure that the power fed into the main grid falls within the allowed range.

Step 4: after the operation day, JODC calculates the revenue of each participant in the WF-FLJOS, taking into account the actual wind power output and the performance of the loads. Detailed participation methods are discussed in Section III-C.

This paper considers the following factors: ① the main grid requirements on wind farm schedule curves, as given in Section III-A, are used as the evaluation criterion; and ② considering the time required for the decision making and communication between JODC and the loads, the JODC issues regulation commands to the loads a short time before the actual operating point based on ultra-short-term wind power forecast information.

C. Participation Methods of Flexible Loads Under Joint Operation Model

The flexible loads in the WF-FLJOS realize the ability to be supplied by both the DN and the wind farm, which is the most significant difference from the traditional demand response model. Therefore, the flexible loads can utilize the power balancing mechanism of the DN to increase the equivalent adjustable capacity provided to the wind farm. The JODC organizes load signing agreements, with the details of the agreements depending on the type of load and business. Small capacity loads, such as TCLs, participate in WF-FLJOS through load agents. The JODC signs agreements with the agents and issues regulation instructions to the agent level. The response and distribution of commands are internal affairs of the load agent and the wind farm does not interfere with these processes. This subsection discusses the participation methods of TCL agent and MG in the WF-FLJOS.

1) TCL Agent

Assuming that the TCL agent chooses to participate in auxiliary declaration business, wind curtailment mitigation business, and clean power supply business. The agreement between JODC and TCL agent includes: ① the timeframe for each business; ② the adjustable capacity range for each interval; and ③ the wind power supply price. To encourage flexible loads to absorb more wind power, the unit price of electricity supplied by the wind farm to the TCL agent adopts a stepped descending curve. As the TCL agent consumes more wind power, the unit electricity purchase cost decreases. The revenue of the wind farm from selling electricity to the TCL agent at time t $C_t^{\text{wf,tcl}}$ can be written as:

$$C_t^{\text{wf,tcl}}=\begin{cases} c_t^{\text{tcl},1}P_t^{\text{w2tcl}}\Delta t \quad L_t^{\text{tcl,min}}\leq P_t^{\text{w2tcl}}<L_t^{\text{tcl},1} \\ [c_t^{\text{tcl},1}L_t^{\text{tcl},1}+c_t^{\text{tcl},2}(P_t^{\text{w2tcl}}-L_t^{\text{tcl},1})]\Delta t \\ \qquad L_t^{\text{tcl},1}\leq P_t^{\text{w2tcl}}<L_t^{\text{tcl},2} \\ [c_t^{\text{tcl},1}L_t^{\text{tcl},1}+c_t^{\text{tcl},2}(L_t^{\text{tcl},2}-L_t^{\text{tcl},1})+c_t^{\text{tcl},3}(P_t^{\text{w2tcl}}-L_t^{\text{tcl},2})]\Delta t \\ \qquad L_t^{\text{tcl},2}\leq P_t^{\text{w2tcl}}\leq L_t^{\text{tcl,max}} \end{cases} \tag{3}$$

The detailed calculation of $L_t^{\text{tcl,min}}$ is presented in (A1) in Appendix A.

2) MG

In the grid-connected mode, MGs can participate in joint operation model to fully utilize internal resources and improve the operation revenue. Instead of arranging energy management within the MG, JODC makes scheduling decisions based on information provided in the contract, such as the electricity prices and generation output limits. We assume that MG chooses to participate in auxiliary declaration business and wind curtailment mitigation business. The agreement between JODC and MG is similar to that of the TCL agent, except that MG can both absorb wind power and utilize internal generation sources to supply power to the wind farm-grid connection point.

Transactions between the wind farm and MGs are based on stepped tariffs. MGs can provide bidirectional power supply. Moreover, the unit price of wind power decreases as MGs increase their power consumption. If MGs provide more reverse power, higher compensation costs are required. The revenue of wind farm from selling electricity to MG at time t $C_t^{\text{wf,mg}}$ can be written as:

$$C_t^{\text{wf,mg}} = C_t^{\text{wf,mg,+}} - C_t^{\text{wf,mg,-}} \tag{4}$$

$$C_t^{\text{wf,mg,+}} = \begin{cases} c_t^{\text{mg,+,1}} P_t^{\text{w2mg}} \Delta t & 0 \le P_t^{\text{w2mg}} < \Delta L_t^{\text{mg,+}} \\ [c_t^{\text{mg,+,1}} \Delta L_t^{\text{mg,+}} + c_t^{\text{mg,+,2}} (P_t^{\text{w2mg}} - \Delta L_t^{\text{mg,+}})] \Delta t & \Delta L_t^{\text{mg,+}} \le P_t^{\text{w2mg}} < 2\Delta L_t^{\text{mg,+}} \\ [(c_t^{\text{mg,+,1}} + c_t^{\text{mg,+,2}} - 2c_t^{\text{mg,+,3}}) \Delta L_t^{\text{mg,+}} + c_t^{\text{mg,+,3}} P_t^{\text{w2mg}}] \Delta t & 2\Delta L_t^{\text{mg,+}} \le P_t^{\text{w2mg}} < L_t^{\text{mg,max,+}} \end{cases} \tag{5}$$

The expression of $C_t^{\text{wf,mg,-}}$ is similar to (5) and is not further elaborated here.

D. Settlement on Load Side Under Joint Operation Model

The equivalent cost for flexible loads in WF-FLJOS comprises the cost of purchasing electricity from the DN, the cost of trading with the wind farm, and violation penalties. If the actual response of the load exceeds the allowed range and causes the wind farm to be penalized by the main grid, JODC may charge the load for the penalty. The actual regulation of the load is measured by the smart meter installed on the distribution line connecting the load side to the wind farm. The electricity price and the cost settlement period are determined through mutual agreement. To address uncertainties in load response, this study designs a dispatch-feedback-response mechanism for the load side to respond to JODC commands. Accordingly, the penalty mechanism on the load side is analyzed.

Figure 2 shows the calculation of load response deviation penalty cost. JODC sends an initial command P_t^{com} to the flexible load based on the adjustable range constraints in the contract. After receiving the initial command, the load confirms and feeds back its achievable value P_t^{cof} to JODC. If the load does not feed back P_t^{cof}, the JODC defaults to the achievable value of the load being equal to P_t^{com}. This process aims to mitigate the risk of non-compliance with the adjustable capacity constraint in the contract due to its response uncertainty. JODC calculates the actual response deviation rate Δ_t^{act} for each load and compares it to the allowed deviation rate Δ_t^{per}. If $\Delta_t^{\text{act}} > \Delta_t^{\text{per}}$ and the wind farm incurs a deviation penalty cost $C_t^{\text{wf,dev}}$ from the main grid, the load is required to pay a penalty to JODC. The penalty for load is denoted as $C_t^{\text{fl,dev}}$. The corresponding violation power equals to the smaller of the wind power deviation to main grid $P_t^{\text{wf.dev}}$ and the response deviation on the load side $|P_t^{\text{cof}} - P_t^{\text{act}}|$. We set P_t^{act} as the actual response value of the load. The deviation penalty factor for loads is represented as $\lambda_t^{\text{fl,dev}}$. In addition, in order to prevent the wind power producer from profiting by penalties, $\lambda_t^{\text{fl,dev}}$ should not be higher than the deviation penalty factor of the wind farm.

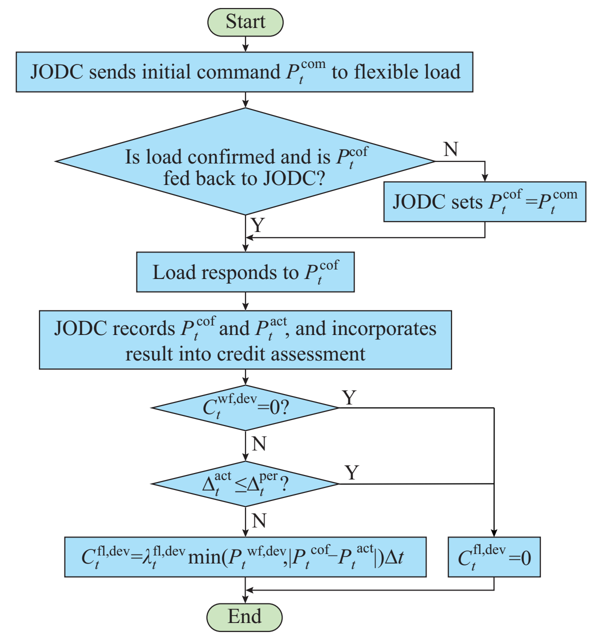

Fig. 2. Calculation of load response deviation penalty cost.

The flexible load and the wind farm are in a cooperative relationship. Therefore, if the wind farm is not penalized for deviation, even if Δ_t^{act} exceeds the limit, the flexible load is not charged for the penalty. Nevertheless, the JODC incorporates such occurrences into the long-term credit assessment to guide and improve the cooperative environment in the WF-FLJOS. If $P_t^{\text{cof}} < P_t^{\text{com}}$, it indicates that the available capacity range of the flexible load specified in contract is inaccurate. Hence, the JODC records P_t^{cof} and incentivizes the load side to submit a more accurate available capacity range by correcting the available capacity or compensation price of the load. For instance, the JODC may provide wind power at a lower price to loads with a more accurate available capacity range.

IV. Joint Operation Model of WF-FLJOS

Based on the analysis of the power supply agreement on the load side, this section establishes a joint operation model of WF-FLJOS under multiple time scales by considering the uncertainty of wind power.

A. Day-ahead Schedule Declaration Model of WF-FLJOS on Main Grid Side

The stochastic optimization approach is applied to the day-ahead schedule declaration model of WF-FLJOS on the main grid side, which is aimed to maximize the revenue of the wind farm. If the distribution line between the wind farm and the flexible load is owned by the DN operator, the WF-FLJOS can obtain the right to use it by leasing or purchasing. If it belongs to the WF-FLJOS, the corresponding construction and maintenance cost sharing ratio can be negotiated among the participants. This study assumes that the distribution lines and transformers are constructed and maintained by the wind farm, and no network costs are charged to the flexible loads. Active power losses of distribution lines and transformers are not considered. Maintenance costs for distribution lines and transformers are settled annually and are not included in the following objective functions. The corresponding formula can be found in [25]. It is worth noting that the purpose of day-ahead schedule declaration model is to obtain the schedule curve. The data on revenues of wind farm and penalties are not actual values and do not serve as a basis for subsequent revenue settlement. The decision variable is the schedule wind power output of the wind farm at the day-ahead stage. The day-ahead schedule declaration model of WF-FLJOS on main grid side can be represented in (6)-(14). In addition, the distribution line capacity constraints should be included.

$$\max \sum_{s \in S_{\mathrm{da}}} \tau_s \sum_{t \in T} (C^{\mathrm{wg}}_{t,s,\mathrm{da}} + C^{\mathrm{wd}}_{t,s,\mathrm{da}} - C^{\mathrm{wc}}_{t,s,\mathrm{da}} - C^{\mathrm{dev}}_{t,s,\mathrm{da}}) \tag{6}$$

s.t.

$$C^{\mathrm{wg}}_{t,s,\mathrm{da}} = c^{\mathrm{g}}_t P^{\mathrm{wg}}_{t,s,\mathrm{da}} \Delta t \tag{7}$$

$$C^{\mathrm{wd}}_{t,s,\mathrm{da}} = C^{\mathrm{wf,tcl}}_{t,s,\mathrm{da}} + C^{\mathrm{wf,mg}}_{t,s,\mathrm{da}} \tag{8}$$

$$C^{\mathrm{wc}}_{t,s,\mathrm{da}} = c^{\mathrm{wc}}_t P^{\mathrm{wc}}_{t,s,\mathrm{da}} \Delta t \tag{9}$$

$$C^{\mathrm{dev}}_{t,s,\mathrm{da}} = (\lambda^{\mathrm{dev,sup}}_t P^{\mathrm{dev,sup}}_{t,s,\mathrm{da}} + \lambda^{\mathrm{dev,ins}}_t P^{\mathrm{dev,ins}}_{t,s,\mathrm{da}}) \Delta t \tag{10}$$

$$P^{\mathrm{wg}}_{t,s,\mathrm{da}} = P^{\mathrm{w2g}}_{t,s,\mathrm{da}} + P^{\mathrm{mg2w}}_{t,s,\mathrm{da}} \tag{11}$$

$$\begin{cases} P^{\mathrm{dev,sup}}_{t,s,\mathrm{da}} = \max(P^{\mathrm{wg}}_{t,s,\mathrm{da}} - (1+\alpha_{\mathrm{da}}) P^{\mathrm{ws}}_{t,\mathrm{da}}, 0) \\ P^{\mathrm{dev,ins}}_{t,s,\mathrm{da}} = \max((1-\beta_{\mathrm{da}}) P^{\mathrm{ws}}_{t,\mathrm{da}} - P^{\mathrm{wg}}_{t,s,\mathrm{da}}, 0) \end{cases} \tag{12}$$

$$0 \le P^{\mathrm{ws}}_{t,\mathrm{da}} \le P^{\mathrm{w,max}} \tag{13}$$

$$P^{\mathrm{wa}}_{t,s,\mathrm{da}} = P^{\mathrm{w2g}}_{t,s,\mathrm{da}} + P^{\mathrm{w2tcl}}_{t,s,\mathrm{da}} + P^{\mathrm{w2mg}}_{t,s,\mathrm{da}} + P^{\mathrm{wc}}_{t,s,\mathrm{da}} \tag{14}$$

where subscript da denotes day-ahead stage.

B. Intraday Schedule Correction Model of WF-FLJOS on Main Grid Side

Allowing wind farms to make frequent schedule revisions during the day helps to improve their operation revenues. However, this practice inevitably increases the pressure on the main grid to make schedule adjustments. Conversely, if wind farms are required to operate strictly according to the day-ahead schedule curve, the operation revenues on farm side will be adversely affected. The accuracy of wind power forecast at the intraday stage is significantly higher than the day-ahead wind power forecast, and part of the uncertainty component can be absorbed by flexible loads. Therefore, in order to balance the operation revenue of the wind farm and the adjustment cost of the main grid, this study allows the wind farm to make a single correction to the day-ahead schedule 2 hours before the operating point at the intraday stage. The objective of the wind farm is to obtain the intraday schedule correction model of WF-FLJOS on the main grid side and maximize its operation revenue.

$$\max \sum_{s \in S_{\mathrm{id}}, t = t_0 + 2} \tau_s \, (C^{\mathrm{wg}}_{t,s,\mathrm{id}} + C^{\mathrm{wd}}_{t,s,\mathrm{id}} - C^{\mathrm{wc}}_{t,s,\mathrm{id}} - C^{\mathrm{dev}}_{t,s,\mathrm{id}} - C^{\mathrm{pen}}_{t,\mathrm{id}}) \tag{15}$$

$$\begin{aligned} C^{\mathrm{pen}}_{t,\mathrm{id}} = {} & \lambda^{\mathrm{pen,sup}(')}_t u^{\mathrm{sup}}_t (P^{\mathrm{ws}}_{t,\mathrm{id}} - P^{\mathrm{ws}}_{t,\mathrm{da}}(P^{\mathrm{ws}'}_t))\Delta t + \\ & \lambda^{\mathrm{pen,ins}(')}_t u^{\mathrm{ins}}_t (P^{\mathrm{ws}}_{t,\mathrm{da}}(P^{\mathrm{ws}'}_t) - P^{\mathrm{ws}}_{t,\mathrm{id}})\Delta t \end{aligned} \tag{16}$$

$$u^{\mathrm{sup}}_t = \begin{cases} 0 & (1+\alpha_{\mathrm{id}}) P^{\mathrm{ws}}_{t,\mathrm{id}} < (1+\alpha_{\mathrm{da}})(1-v^{\mathrm{res}}_t) P^{\mathrm{ws}}_{t,\mathrm{da}} + (1+\alpha_{\mathrm{res}}) v^{\mathrm{res}}_t P^{\mathrm{ws}'}_t \\ 1 & \text{otherwise} \end{cases} \tag{17}$$

$$u^{\mathrm{ins}}_t = \begin{cases} 0 & (1-\beta_{\mathrm{id}}) P^{\mathrm{ws}}_{t,\mathrm{id}} > (1-\beta_{\mathrm{da}})(1-v^{\mathrm{res}}_t) P^{\mathrm{ws}}_{t,\mathrm{da}} + (1-\beta_{\mathrm{res}}) v^{\mathrm{res}}_t P^{\mathrm{ws}'}_t \\ 1 & \text{otherwise} \end{cases} \tag{18}$$

C. Real-time Predictive Control Model of WF-FLJOS on Main Grid Side

The JODC formulates and issues dispatch commands to the flexible loads per minute. If the wind power output meets the deviation requirement, JODC does not dispatch the flexible load. The assessment criterion is whether the actual total deviation of wind power of a 5 min interval exceeds the allowed range. Therefore, in each interval, the dispatch commands on the load side in the current and subsequent intervals should be arranged based on the amount of deviation that has occurred. However, only the control commands for the current interval are issued. The real-time accuracy of the wind power forecast is relatively high. Thus, the forecast value after a short-time interval (on the second-level time scale) is considered to be equal to the actual maximum generatable power of the wind farm. The power at subsequent points within the assessment period can be obtained by means of the moving average method. Decision variables include the dispatch commands to flexible loads and the wind power input to main grid in the current interval. The objective is to use the intraday schedule as a reference, control the wind power output to meet the assessment requirements, and ensure the economic operation of the wind farm. In (19)-(21), we set $t_{\mathrm{rt,s}} = i\Delta t' + (4-n)\Delta t''$, $t_{\mathrm{rt,e}} = i\Delta t' + 4\Delta t''$, and $t_{\mathrm{rt,0}} = i\Delta t'$, where n takes values from 4 to 0 in sequence, representing the number of 1 min intervals between the current operating point and the adjacent next 5 min segmentation point. In (20) and (21), the first term is the deviation power in the current and forward intervals, and the second term is the power difference between the total allowed deviation of a 5 min interval and the deviation that has occurred.

$$\min_{t_{\mathrm{rt}} \in [t_{\mathrm{rt,s}}, t_{\mathrm{rt,e}}]} (P^{\mathrm{dev,sup}}_{t_{\mathrm{rt}}} + P^{\mathrm{dev,ins}}_{t_{\mathrm{rt}}}) \tag{19}$$

$$\begin{aligned} P^{\mathrm{dev,sup}}_{t_{\mathrm{rt}}} = \max\Bigg(& \sum_{t'_{\mathrm{rt}} = t_{\mathrm{rt,s}}}^{t_{\mathrm{rt,e}}} |P^{\mathrm{wg}}_{t'_{\mathrm{rt}}} - P^{\mathrm{ws}}_{t_{\mathrm{rt,id}}}| \delta^{\mathrm{sup}}_{t'_{\mathrm{rt}}} - \max\Bigg(\alpha_{\mathrm{id}} \sum_{t'_{\mathrm{rt}} = t_{\mathrm{rt,0}}}^{t_{\mathrm{rt,e}}} P^{\mathrm{ws}}_{t_{\mathrm{rt,id}}} - \\ & \sum_{t'_{\mathrm{rt}} = t_{\mathrm{rt,0}}}^{t_{\mathrm{rt,s}}} |P^{\mathrm{wg}}_{t'_{\mathrm{rt}}} - P^{\mathrm{ws}}_{t_{\mathrm{rt,id}}}| \delta^{\mathrm{sup}}_{t'_{\mathrm{rt}}}, 0 \Bigg), 0 \Bigg) \end{aligned} \tag{20}$$

$$\begin{aligned} P^{\mathrm{dev,ins}}_{t_{\mathrm{rt}}} = \max\Bigg(& \sum_{t'_{\mathrm{rt}} = t_{\mathrm{rt,s}}}^{t_{\mathrm{rt,e}}} |P^{\mathrm{ws}}_{t_{\mathrm{rt,id}}} - P^{\mathrm{wg}}_{t'_{\mathrm{rt}}}| \delta^{\mathrm{ins}}_{t'_{\mathrm{rt}}} - \max\Bigg(\beta_{\mathrm{id}} \sum_{t'_{\mathrm{rt}} = t_{\mathrm{rt,0}}}^{t_{\mathrm{rt,e}}} P^{\mathrm{ws}}_{t_{\mathrm{rt,id}}} - \\ & \sum_{t'_{\mathrm{rt}} = t_{\mathrm{rt,0}}}^{t_{\mathrm{rt,s}}} |P^{\mathrm{ws}}_{t_{\mathrm{rt,id}}} - P^{\mathrm{wg}}_{t'_{\mathrm{rt}}}| \delta^{\mathrm{ins}}_{t'_{\mathrm{rt}}}, 0 \Bigg), 0 \Bigg) \end{aligned} \tag{21}$$

Figure 3 illustrates the decision-making process of JODC at the real-time stage. Assume that the current interval t_0 is within the third segment of the 5 min interval. The two intervals before t_0 are denoted as previous intervals, and the two intervals after t_0 are denoted as look-ahead intervals. JODC calculates the positive and negative deviations that have occurred in $t_0-\Delta t''$ and $t_0-2\Delta t''$, then subtracts them from the total allowed deviation in 5 min to obtain the allowed deviation in the remaining three time intervals. JODC takes (19) as the control objective and dispatches the loads sequentially, in descending order of the wind power supply cost or in ascending order of the reverse supply cost in the contracts. After receiving the command, the flexible load can confirm the capacity for response and provide feedback to the JODC. If the confirmed capacity of a load is less than the command value, JODC reallocates the shortfall to other loads in sequence until the power balance constraint is satisfied. Meanwhile, the participating loads respond to the confirmed capacity at the actual operating point. Following these steps, the wind power integrated into grid and the interactive power with the flexible loads can be obtained for each interval.

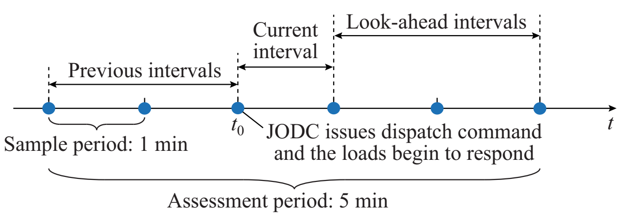

Fig. 3. Decision-making process of JODC at real-time stage.

The the real-time forecast control algorithm (pseudocode) is presented in Algorithm 1.

Algorithm 1: real-time forecast control algorithm (pseudocode)

Input: $P^{\mathrm{ws}}_{t,\mathrm{id}}$, c^{g}_t, $c^{\mathrm{tcl},k}_t$, $c^{\mathrm{mg},r}_t$, and available capacity of flexible loads
Output: $P^{\mathrm{w2tcl}}_{t_{\mathrm{rt}}}$, $P^{\mathrm{mg}}_{t_{\mathrm{rt}}}$, $P^{\mathrm{mg2w}}_{t_{\mathrm{rt}}}$, and $P^{\mathrm{wg}}_{t_{\mathrm{rt}}}$
for $i=1,2,\ldots,288$ **do**
  for $n=5,4,\ldots,1$ **do**
  Predict the maximum wind power output of wind farm in day-ahead and current intervals
  Sort wind power supply price and reverse power supply price on load side
  Calculate positive and negative allowed power deviation in 5 min, which are $\alpha_{\mathrm{id}}\sum_{t'_{\mathrm{rt}}=t_{\mathrm{rt},0}}^{t_{\mathrm{rt},e}} P^{\mathrm{ws}}_{t'_{\mathrm{rt},\mathrm{id}}}$ and $\beta_{\mathrm{id}}\sum_{t'_{\mathrm{rt}}=t_{\mathrm{rt},0}}^{t_{\mathrm{rt},e}} P^{\mathrm{ws}}_{t'_{\mathrm{rt},\mathrm{id}}}$, respectively
  Calculate positive and negative deviations that occur in 5 min, which are $\sum_{t'_{\mathrm{rt}}=t_{\mathrm{rt},0}}^{t_{\mathrm{rt},s}} |P^{\mathrm{wg}}_{t'_{\mathrm{rt}}}-P^{\mathrm{ws}}_{t'_{\mathrm{rt},\mathrm{id}}}|\delta^{\mathrm{sup}}_{t'_{\mathrm{rt}}}$ and $\sum_{t'_{\mathrm{rt}}=t_{\mathrm{rt},0}}^{t_{\mathrm{rt},s}} |P^{\mathrm{ws}}_{t'_{\mathrm{rt},\mathrm{id}}}-P^{\mathrm{wg}}_{t'_{\mathrm{rt}}}|\delta^{\mathrm{ins}}_{t'_{\mathrm{rt}}}$, respectively
  Calculate positive and negative allowed power deviation in current and look-ahead intervals, which are $\max\left(\alpha_{\mathrm{id}}\sum_{t'_{\mathrm{rt}}=t_{\mathrm{rt},0}}^{t_{\mathrm{rt},e}} P^{\mathrm{ws}}_{t'_{\mathrm{rt},\mathrm{id}}} - \sum_{t'_{\mathrm{rt}}=t_{\mathrm{rt},0}}^{t_{\mathrm{rt},s}} |P^{\mathrm{wg}}_{t'_{\mathrm{rt}}}-P^{\mathrm{ws}}_{t'_{\mathrm{rt},\mathrm{id}}}|\delta^{\mathrm{sup}}_{t'_{\mathrm{rt}}},0\right)$ and $\max\left(\beta_{\mathrm{id}}\sum_{t'_{\mathrm{rt}}=t_{\mathrm{rt},0}}^{t_{\mathrm{rt},e}} P^{\mathrm{ws}}_{t'_{\mathrm{rt},\mathrm{id}}} - \sum_{t'_{\mathrm{rt}}=t_{\mathrm{rt},0}}^{t_{\mathrm{rt},s}} |P^{\mathrm{ws}}_{t'_{\mathrm{rt},\mathrm{id}}}-P^{\mathrm{wg}}_{t'_{\mathrm{rt}}}|\delta^{\mathrm{ins}}_{t'_{\mathrm{rt}}},0\right)$, respectively
  Substitute $P^{\mathrm{dev,sup}}_{t_{\mathrm{rt}}}$ and $P^{\mathrm{dev,ins}}_{t_{\mathrm{rt}}}$ into (19)
  JODC issues dispatch commands to flexible loads based on sorting order and obtains grid-connected wind power for current interval
  end
end

V. Case Studies

This section investigates the effectiveness and performance of the WF-FLJOS. All simulations are implemented in Python with Gurobi solver. The installed capacity of the wind farm is 100 MW, and the forecast and actual wind power output data from EirGrid on October 28, 2020 [26] are used and converted to the required size. The wind power scenarios are simulated based on the statistical distribution of wind power forecast error and fluctuation [27]. Table I shows the purchasing and selling price of electricity. In the agreements between JODC and flexible loads, the purchase of electricity from the wind farm and the sale of electricity to the wind farm-grid connection point adopt the time-of-use (TOU) pricing format. Other simulation parameters are given in [25].

TABLE I
Purchasing and Selling Prices of Electricity

Period	Time duration	Purchasing price (¥/kWh)	Selling price (¥/kWh)
Peak	10:00-12:00, 14:00-19:00	1.10	0.8
Valley	00:00-08:00	0.35	0.2
Flat	08:00-10:00, 12:00-14:00, 19:00-24:00	0.65	0.4

A. Operation Results of WF-FLJOS

Figure 4 shows the relationship between the maximum actual wind power output, the actual wind power output to the main grid, and the allowed range of the wind farm on multiple time scales. The interval is set to be 5 min.

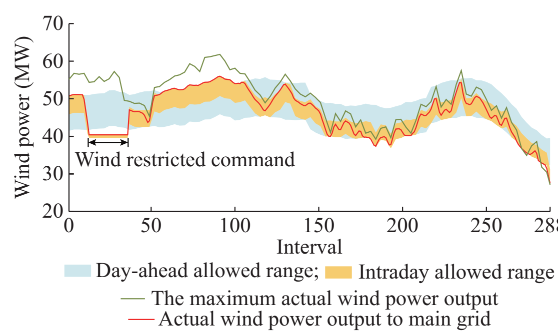

Fig. 4. Relationship between the maximum actual wind power output, actual wind power output to main grid, and allowed range of wind farm on multiple time scales.

The main grid operator issues the wind-restricted command at the intraday stage, requesting that the wind power output does not exceed 40 MW between 01:00 and 03:00. The allowed deviation rate for the day-ahead schedule is ±10%, while the allowed deviation rates at wind-restricted and wind-unrestricted stages at intraday stage are ±1% and ±5%, respectively. Due to the limited accuracy of the forecast wind power at the day-ahead stage, the wind farm needs to adjust its schedule wind power output at the intraday stage. Therefore, in intervals 182-186, 191-195, and 287-288, the intraday allowed range exceeds the boundaries of the day-ahead allowed range, resulting in a penalty of ¥665 paid by the wind farm to the main grid. It is worth noting that the actual wind power output falls within the intraday allowed range, ensuring that the main grid has sufficient capacity to compensate for the deviation.

In intervals 13-32, which are at the wind-restricted stage, JODC utilize the entire upward regulation capacity of both the TCL agent and MG, yet there is still 4.074 MWh curtailed wind power. In intervals 1-12 and 55-102, the available wind power significantly exceeds the day-ahead schedule curve. After intraday adjustments, the allowed boundaries for these intervals align precisely with the day-ahead allowed ranges. This alignment effectively maximizes the potential revenue from wind power sales. Simultaneously, there is no curtailed wind power because the upward capacity is sufficient in these intervals.

The power composition of the TCL agent is shown in Fig. 5. The interval is set to be 5 min. The TCL loads are supplied by both the DN and the wind farm. The power supply from the DN is denoted as "DN supply", and the power supply from the wind farm is denoted as "wind farm supply". In the contract, the allowed range of clean power supply business in interval t is set as $[L_t^{\text{tcl,min}}, L_t^{\text{tcl,1}}]$. If the wind power supplied to the TCL agent is less than $L_t^{\text{tcl,1}}$, the TCL agent may increase the purchasing power from the DN to meet the minimum energy demand of the TCL loads, which corresponds to "DN supplements" in Fig. 5. If the power supplied to TCL agent reaches $L_t^{\text{tcl,min}}$ while the wind power supply to the main grid is still insufficient, JODC may dispatch the MG.

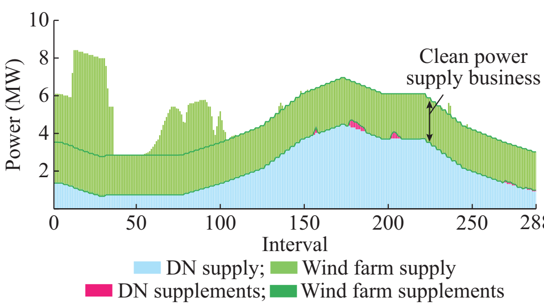

Fig. 5. Power consumption of TCL agent.

Figure 6 shows the dispatch commands from JODC to MG. The interval is set to be 5 min. In intervals 177-187, the wind farm reduces the power supplied to the TCL agent. The wind power injected into the main grid satisfies the deviation requirement in intervals 185-187. As a result, there is no necessity to dispatch the MG. In intervals 13-32, even after the JODC fully utilizes the available load capacity, there remains a surplus of the wind power. This prompts the TCL agent to reduce the power purchased from the DN to absorb more wind power. This part of wind power consumption corresponds to the "wind farm supplements" in Fig. 5. It can be observed that JODC can utilize the flexible power supply contracts signed with the loads to organize dispatch commands effectively.

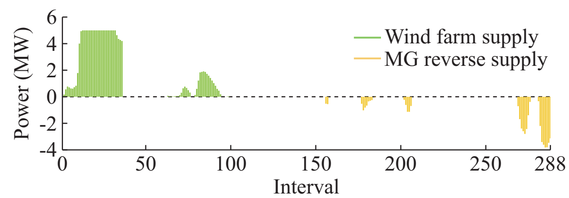

Fig. 6. Dispatch commands from JODC to MG.

The following five cases are compared to demonstrate the advantages of WF-FLJOS and the factors that affect the costs on the load side and the farm side. The detailed settings of the cases are as follows.

Case 1: TCL agent, MG, and wind farm all operate independently.

Case 2: TCL agent and wind farm participate in joint operation.

Case 3: TCL agent, wind farm, and MG participate in joint operation, and TCL agent participates in auxiliary declaration business and wind curtailment mitigation business.

Case 4: based on case 3, the TCL agent also participates in clean power supply business, but the balancing capability for power fluctuation of DN is ignored.

Case 5: the enhanced scheduling strategy proposed in this paper.

Table II compares the optimization results of different cases, where Q_c^{wc} is the amount of curtailed wind power. It is worth noting that $\Delta C_c^{\text{WF-FLJOS}}$ is equal to the difference between the joint operation revenue and the revenue in case 1.

TABLE II
OPTIMIZATION RESULTS OF DIFFERENT CASES

Case No.	$C_c^{\text{wf,tcl}}$ (10^3 ¥)	C_c^{tcl} (10^3 ¥)	C_c^{pen} (10^3 ¥)	$C_c^{\text{wf,mg}}$ (10^3 ¥)	Q_c^{wc} (MWh)	C_c^{wf} (10^3 ¥)	$\Delta C_c^{\text{WF-FLJOS}}$ (10^3 ¥)
1	0	122.32	13.978	0	39.860	490.12	0
2	33.85	77.31	1.789	0	13.598	518.28	73.17
3	7.42	81.96	0.189	−1.62	6.790	515.56	65.80
4	29.76	77.34	0.368	−1.37	4.364	520.55	75.41
5	32.90	76.73	0.354	−0.89	4.099	521.42	76.89

In case 1, the wind farm and TCL agent both operate independently. The wind farm submits the forecast power before the day and corrects the forecast curve with the updated value during the day. Due to the lack of adjustable resources, the wind farm faces higher penalties for schedule revisions and output deviations, resulting in the lowest revenue in this case. The power consumption of the TCL agent equals the power required by the TCLs to maintain their preferred temperatures, which is entirely supplied by the DN. The power consumption of the TCL agent cannot be adjusted, and the selling price of electricity of DN is higher than what the wind farm offers in the joint operation, so the TCL agent has the highest power cost in case 1.

In case 2, the TCL agent can consume the wind power to reduce its electricity cost. The TCL agent does not have the ability to provide reverse power, so it has limited downward adjustable capacity. Consequently, JODC needs to make significant corrections to the intraday schedule curve to minimize the output deviation. As there is only one electricity buyer on the load side under the joint operation model, the revenue of the wind farm decreases by ¥3.14×10^3 compared with case 5. The incremental revenue for case 2 is ¥73.17×10^3, which benefits from the lower cost of TCL agent and the increased revenue of the wind farm.

Compared with case 5, the TCL agent in case 3 does not participate in the clean power supply business. Hence, the TCL agent has to purchase more electricity from the DN, which increases the electricity cost and decreases the wind farm revenue. This comparison proves that single business may limit the revenue growth potential of the participants.

In case 4, the adjustable capacities of the TCL agents rely solely on their inherent flexibility. The capacity of the clean power supply business in interval t equals to $L_t^{\mathrm{tcl,min}}$, which is lower than that in case 5. Thus, the cost of the TCL agent increases. Since the TCL agent cannot provide $P_t^{\mathrm{tcl,b1}}$ when the wind power is insufficient, JODC is compelled to purchase more reverse electricity from MG, thereby further reducing the revenue of the wind farm. This shows that the flexible loads can utilize the dual-source power supply capacity to reduce their own costs and provide more benefits to the wind farm.

In cases where the wind farm is large and the available capacity provided by flexible loads is limited, the adjustable capacity on the load side may not be sufficient to fully compensate for output deviations. Therefore, the following two cases are designed to investigate the impact of flexible load adjustable capacity on the operation of the WF-FLJOS.

Case 6: based on case 5, the total amount of TCLs included in the TCL agent is multiplied by factors ranging from 0 to 4, and the available capacity of the MG is multiplied by factors ranging from 0 to 3.

Case 7: the TCL agent does not participate in the clean power supply business, while the other parameters are the same as in case 6.

The relationship between the available capacities of TCL agent and MG and the revenue of wind farm is shown in Fig. 7. The multiplicative factors for two types of flexible loads are denoted as k_{tcl} and k_{mg}, respectively. Surfaces A and B represent the operation results of cases 6 and 7, respectively. If neither TCL agent nor MG participates in the joint operation, the wind farm revenue is ¥507.48×10^3. As the available capacities of two types of flexible loads increase, the daily operation revenue of the wind farm also rises. When the available capacity of TCL agent remains constant and the MG capacity is already substantial and continues to increase, the operation revenue of the wind farm tends to be stable. This is because the price of electricity sold by the wind farm to the MG is lower than that sold to the main grid, and the MG primarily serves to balance power deviations. If flexible loads can cover wind power deviation, further increasing the capacity of MG will have a limited impact on wind farm profitability. In case 6, when $k_{\mathrm{tcl}}=4$, even if k_{mg} increases from 2 to 4, the revenue of the wind farm remains at 542.175×10^3 RMB. Comparing surfaces A and B in Fig. 7, it can be seen that the revenue of wind farm is related to the business type of flexible loads. As k_{tcl} increases, the revenue growth of the wind farm in case 6 is larger than that in case 7. This is because in clean power supply business, the selling price of electricity from wind farm to TCL agent is higher than the feed-in tariff of wind power. Therefore, the wind farm increases the power supply to TCL agent and improve its revenue.

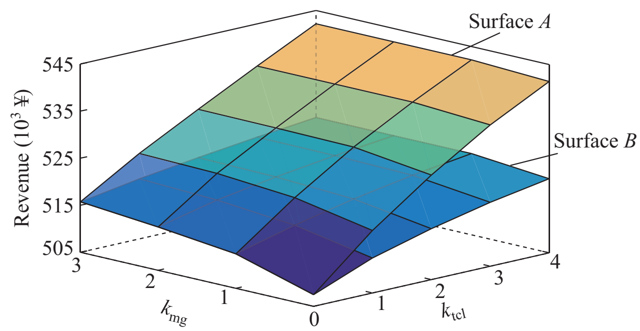

Fig. 7. Relationship between available capacities of TCL agent and MG and revenue of wind farm.

Figure 8 illustrates the relationship between the available capacity of flexible loads and curtailed wind power. The amount of curtailed wind power decreases significantly as the available capacity of flexible loads increases. In case 6, TCL agent absorbs more wind power which results in less curtailed wind power curtail for the same multiplicative factors.

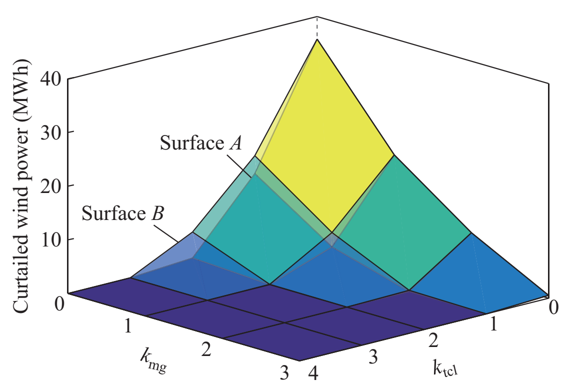

Fig. 8. Relationship between available capacities of flexible loads and curtailed wind power.

From the above analysis, it is evident that factors such as the type of flexible load, adjustable capacity, and business models can affect the operation performance of the WF-FLJOS.

B. Comparison of Different Intraday Schedule Correction Modes for Wind Farm

Since the main grid operator issues wind-restricted commands during the day, only the total amount and frequency of schedule adjustments at wind-unrestricted stage are considered in this study. The main grid schedule adjustment cost refers to the correction costs of other resources due to the wind farm revising its schedule wind power output at the intraday stage. The adjustment cost of the main grid increases as the actual operating point approaches. In this study, the average adjustment cost on the grid side ranges from 15 min to 4 hours before the actual operating point is between $400\gamma_1$ ¥/MWh and $100\gamma_2$ ¥/MWh, where γ_1 and γ_2 are the cost factors. The unit adjustment cost for each interval is derived by interpolation. The optimization results in different correction modes are shown in Table III, where $W^{\mathrm{c,sum}}$ is the total amount of corrections made by the wind farm during the day; and $f^{\mathrm{c,sum}}$ is the total number of corrections.

TABLE III
OPTIMIZATION RESULTS IN DIFFERENT SCHEDULE CORRECTION MODES

Correction mode	$W^{\mathrm{c,sum}}$ (MWh)	$f^{\mathrm{c,sum}}$	$C^{\mathrm{wf,mg}}$ (¥)	C^{wg} (10^3 ¥)	C^{wf} (10^3 ¥)
No-correction	0	0	−8820	493.44	516.26
Rolling correction	200.26	1095	−670	490.27	521.61
Schedule correction	46.18	88	−890	489.97	521.42

No-correction mode means that the wind farm decides its actual wind power output to the main grid according to the day-ahead submission and does not update the intraday schedule curve. Due to the limited accuracy of the day-ahead wind power forecast, this case exhibits the highest reverse power supply from the MG and the lowest benefit for the wind farm.

In the rolling correction mode, wind farms optimize their 15 min to 4 hours schedule wind power outputs every 15 min. The wind power forecast accuracy improves as the actual operating point approaches, and the wind farm can adjust the schedule curve through rolling correction mode to increase the revenue on the farm side. At the intraday stage, the main grid receives the updated wind power plan frequently. The wind farm makes a total of 1095 schedule adjustments on the operation day, with a cumulative quantity of 200.26 MWh. When $\gamma_1=\gamma_2=1.00$, the main grid operator has to pay ¥42.97×10^3 for the schedule adjustment. It can be observed that the rolling correction mode increases the complexity of the operation schedule management for the main grid operator.

By applying the schedule correction mode proposed in this paper, the total correction amount is reduced to 46.18 MWh, and the number of corrections is reduced to 88. The daily revenue of the wind farm is ¥521.42×10^3. Compared with the commonly adopted rolling correction mode, the daily operation revenue of the wind farm decreased by only ¥190. However, the main grid schedule adjustment cost is ¥30.96×10^3 lower than the cost in the rolling correction mode. It is indicative that the schedule correction mode proposed in this paper significantly reduces the main grid regulation burden while only slightly compromising the daily operation revenue on the farm side. Table IV compares the main grid schedule adjustment cost under different regulation cost factors.

TABLE IV
MAIN GRID SCHEDULE ADJUSTMENT COST UNDER DIFFERENT COST FACTORS

γ_1	γ_2	Rolling correction mode (10^3 ¥)	Schedule correction mode (10^3 ¥)	Cost difference (10^3 ¥)
0.25	0.25	10.74	3.00	7.74
0.50	0.80	25.20	6.65	18.55
0.80	0.50	30.66	8.96	21.70
1.00	1.00	42.97	12.01	30.96

The average adjustment cost of the main grid varies in different cases and is influenced by many factors, including the types and total available capacities of adjustable resources. As shown in Table IV, the cost difference between the rolling correction mode and schedule correction mode tends to increase as the average regulation cost rises. Therefore, the schedule correction mode proposed in this paper is more advantageous for the main grid when the adjustable resources on the grid side are limited.

C. Violation Penalty Mechanism of Load Side

As indicated in Section III, when loads participate in joint operation, two types of violations may occur: ① the actual response does not meet the expected quantity after feedback confirmation; and ② the feedback value is lower than the initial regulation instruction issued by JODC. This subsection explores strategy to handle these two cases. To demonstrate the advantage of the proposed strategy of the load side and its impact on operation results, a new MG load is introduced in this case study. The two MG loads are denoted as MG1 and MG2, respectively. In the agreement between JODC and MG2, $L_t^{\mathrm{mg2,max,-}}=0.6$ MW and $c_t^{\mathrm{mg2,-}}=1.9c_t^{\mathrm{g}}$. In addition, the rest of the parameters are the same as MG1.

In case 1, the maximum available wind power falls below the allowed range in intervals 272 and 273. Therefore, JODC issues the reverse power commands to MG loads. MG1 verifies and feeds back the command. If the response capacity of MG1 meets the contracted adjustable capacity, the wind power output of the wind farm to the main grid will fulfill the assessment requirements. Thus, the original deviation of the wind power is zero. However, the actual response capacity of MG1 is 1.8 MW, which is less than the feedback amount. Figure 9 shows the result of MG1 and wind power deviation (case 1). The interval is set to be 5 min. The triangular lines show the mean value of feedback and actual response capacities for each interval. The results indicate that in intervals 272 and 273, the actual wind power deviation to the main grid is 0.794 MW and 0.997 MW, respectively. It is worth noting that MG2 is not dispatched. The main grid imposes ¥268.7 violation penalty to the wind farm. According to Fig. 2, when $\lambda_t^{\mathrm{fl,dev}}=\lambda_t^{\mathrm{dev,ins}}$, MG1 should fully cover the penalty cost.

In case 2, different from case 1, MG1 feeds back the actual response capacity 1.8 MW to JODC. Figure 10 shows the result of MG1, MG2, and wind power deviation (case 2).

The interval is set to be 5 min. Although the actual response capacity of MG1 is insufficient for the initial commands, the JODC can dispatch MG2 in time after receiving the feedback signal from MG1 to compensate for part of the wind power deviation. The results show that the wind power deviation in intervals 272 and 273 is reduced to 0.194 MW and 0.397 MW, respectively, with the corresponding assessment cost decreased to ¥88.65. This violation penalty is paid by the wind farm, but JODC records the accuracy of the feedback quantity of MG1 and incorporates it into the long-term credit assessment.

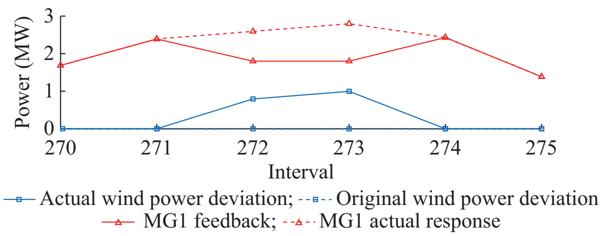

Fig. 9. Result of MG1 and wind power deviation (case 1).

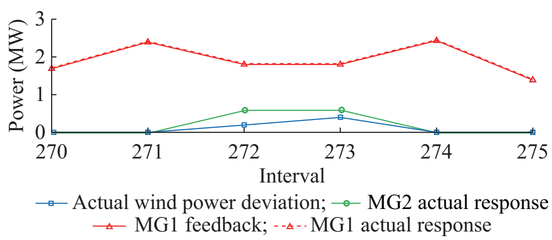

Fig. 10. Result of MG1, MG2, and wind power deviation (case 2).

VI. Conclusion

As the policy gradually encourages wind farms to improve their own regulation capability, it is an important issue how to realize the high-precision tracking of the wind power schedule in an economical and effective way. This paper proposes an enhanced scheduling strategy for WF-FLJOS to resolve part of the uncertainty in the wind power forecast or schedule on the farm side. Compared with the current wind farm operation rules, more stringent assessment requirements on the wind power output accuracy are designed. On this basis, the joint operation model is explored using TCL agent and MG as examples. Considering the uncertainty of the MG response and the cooperative relationship with the wind farm, we design the "dispatch-feedback-response" mechanism for the load side in response to the dispatch commands, including specified penalties for participating loads in cases of violation. Finally, the submission and tracking approach of the generation schedule for the wind farm is established.

Case studies show that the proposed strategy for WF-FLJOS enhances the ability of the wind farm to cope with the output deviation required by the main grid, at both wind-restricted and wind-unrestricted stages. In addition, the proposed strategy reduces the regulation burden on the main grid caused by the widely-used rolling correction mode of power forecast or schedule. Various businesses in WF-FLJOS and the balancing capability provided by the DN are conducive to further enhancing the wind power schedule execution capability and improving the economics of the wind farm and flexible loads. In the future, more types of business models will be considered in the WF-FLJOS.

Appendix A

When the TCLs operate in the cooling mode, the power of the TCL agent cannot be less than $P_t^{\text{tcl,min}}$ to satisfy the minimum needs of the users. The definitions of the symbols are provided in [28].

$$P_t^{\text{tcl,min}} = \sum_{i=1}^{N}\left(\frac{T_t^{\text{out}} - E(T_{i,t}^{\text{set,max}})}{sE(R_i)} - \frac{l}{s}\right) \tag{A1}$$

To reduce the cost of electricity, the agent arranges for part of the power to participate in the clean power supply business, which is denoted as $P_t^{\text{tcl,con,min}}$. $P_t^{\text{tcl,con,min}}$ is the minimum power provided by the wind farm to the TCL agent, which corresponds to the decomposed power for the total amount of clean power supply business in each interval.

If only the adjustable ability of the TCLs is considered, the allowed range of wind power that can be consumed by the agent is $[L_t^{\text{tcl,ori,min}}, L_t^{\text{tcl,ori,max}}]$.

$$\begin{cases} L_t^{\text{tcl,ori,max}} = P_t^{\text{tcl,max}} - P_t^{\text{tcl,min}} + P_t^{\text{tcl,con,min}} \\ L_t^{\text{tcl,ori,min}} = P_t^{\text{tcl,con,min}} \end{cases} \tag{A2}$$

The low-voltage DN has a certain automatic balancing capability for power fluctuations. When the power supply from the wind farm is insufficient, the DN can supplement the deficit to ensure the minimum electricity demand of TCL users. Similarly, if the wind power is surplus, the agent can reduce the power purchased from the DN and increase the acceptance capacity of wind power. Thus, the transferable power consumption from the DN and wind farm can be expressed as (9).

$$P_t^{\text{tcl},b_1} = P_t^{\text{tcl},b_2} = \frac{\alpha_{\text{tcl}}}{1+\alpha_{\text{tcl}}}\left(P_t^{\text{tcl,min}} - P_t^{\text{tcl,con,min}}\right) \tag{A3}$$

In addition, we set $P_t^{\text{tcl},0}$ as the power of TCLs at their preferred temperatures. In the contract, the allowed range and the segmentation points of the stepped curve can be expressed as:

$$\begin{cases} L_t^{\text{tcl,max}} = L_t^{\text{tcl,ori,max}} + P_t^{\text{tcl},b_1} + P_t^{\text{tcl},b_2} \\ L_t^{\text{tcl,min}} = L_t^{\text{tcl,ori,min}} \end{cases} \tag{A4}$$

$$\begin{cases} L_t^{\text{tcl},1} = P_t^{\text{tcl,con,min}} + P_t^{\text{tcl},b_1} \\ L_t^{\text{tcl},2} = P_t^{\text{tcl},0} - P_t^{\text{tcl,min}} + P_t^{\text{tcl,con,min}} + P_t^{\text{tcl},b_1} \end{cases} \tag{A5}$$

Comparing (A2) with (A4), it is indicative that JODC utilizes the power balancing capability of DN to increase the equivalent regulation of wind power output. Moreover, the loads use their inherent flexibility and dual-source power supply mechanism to reduce the impact on their own power consumption.

References

[1] P. Lu, L. Ye, Y. Zhao *et al*., "Review of meta-heuristic algorithms for wind power prediction: methodologies, applications and challenges," *Applied Energy*, vol. 301, p. 117446, Nov. 2021.

[2] J. Shi, W. J. Lee, and X. Liu, "Generation scheduling optimization of wind-energy storage system based on wind power output fluctuation features," in *Proceedings of 2017 IEEE/IAS 53rd Industrial and Commercial Power Systems Technical Conference*, Niagara Falls, Canada, May 2017, pp. 1-7.

[3] L. Yao, B. Yang, H. Cui *et al*., "Challenges and progresses of energy storage technology and its application in power systems," *Journal of Modern Power Systems and Clean Energy*, vol. 4, no. 4, pp. 519-528, Aug. 2016.

[4] H. Bitaraf and S. Rahman, "Reducing curtailed wind energy through energy storage and demand response," *IEEE Transactions on Sustainable Energy*, vol. 9, no. 1, pp. 228-236, Jan. 2018.

[5] X. Chang, Y. Xu, W. Gu *et al*., "Accelerated distributed hybrid stochastic/robust energy management of smart grids," *IEEE Transactions on Industrial Informatics*, vol. 17, no. 8, pp. 5335-5347, Aug. 2021.

[6] C. Zhao, J. Wang, J. P. Watson *et al*., "Multi-stage robust unit commitment considering wind and demand response uncertainties," *IEEE Transactions on Power Systems*, vol. 28, no. 3, pp. 2708-2717, Aug. 2013.

[7] W. Zhang, Y. Xu, W. Liu *et al*., "Distributed online optimal energy management for smart grids," *IEEE Transactions on Industrial Informatics*, vol. 11, no. 3, pp. 717-727, Jun. 2015.

[8] Z. Yuan, P. Li, Z. Li *et al*., "Data-driven risk-adjusted robust energy management for microgrids integrating demand response aggregator and renewable energies," *IEEE Transactions on Smart Grid*, vol. 14, no. 1, pp. 365-377, Jan. 2023.

[9] G. Zhu, Y. Gao, and H. Sun, "Optimization scheduling of a wind – photovoltaic – gas – electric vehicles community-integrated energy system considering uncertainty and carbon emissions reduction," *Sustainable Energy, Grids and Networks*, vol. 33, p. 100973, Mar. 2023.

[10] Southern Regulatory Bureau of the National Energy Administration. (2022, Jun.). Implementation rules for grid-connected operation and ancillary services management of wind power in the southern region. [Online]. Available: http://nfj.nea.gov.cn/xwzx/tzgg/202310/t20231009_140145.html

[11] A. Cerejo, S. Mariano, P. Carvalho *et al*., "Hydro-wind optimal operation for joint bidding in day-ahead market: storage efficiency and impact of wind forecasting uncertainty," *Journal of Modern Power Systems and Clean Energy*, vol. 8, no. 1, pp. 142-149, Jan. 2020.

[12] E. Du, N. Zhang, C. Kang *et al*., "Managing wind power uncertainty through strategic reserve purchasing," *IEEE Transactions on Power Systems*, vol. 32, no. 4, pp. 2547-2559, Jul. 2017.

[13] H. Ding, Z. Hu, and Y. Song, "Rolling optimization of wind farm and energy storage system in electricity markets," *IEEE Transactions on Power Systems*, vol. 30, no. 5, pp. 2676-2684, Sept. 2015.

[14] Y. Mu, H. Li, X. Yu *et al*., "A scenario-based optimal dispatch for joint operation of wind farms and combined heat and power plants considering energy flexibilities in heating networks," *Electric Power Systems Research*, vol. 204, p. 107683, Mar. 2022.

[15] A. Haque, A. I. Saif, P. Nguyen *et al*., "Exploration of dispatch model integrating wind generators and electric vehicles," *Applied Energy*, vol. 183, pp. 1441-1451, Dec. 2016.

[16] B. Qiao and J. Liu, "Multi-objective dynamic economic emission dispatch based on electric vehicles and wind power integrated system using differential evolution algorithm," *Renewable Energy*, vol. 154, pp. 316-336, Jul. 2020.

[17] X. Gao, K. Chan, S. Xia *et al*., "Risk-constrained offering strategy for a hybrid power plant consisting of wind power producer and electric vehicle aggregator," *Energy*, vol. 177, pp. 183-191, Jun. 2019.

[18] Z. Zhang, R. Li, and F. Li, "A novel peer-to-peer local electricity market for joint trading of energy and uncertainty," *IEEE Transactions on Smart Grid*, vol. 11, no. 2, pp. 1205-1215, Mar. 2020.

[19] R. Zhang, T. Jiang, F. Li *et al*., "Coordinated bidding strategy of wind farms and power-to-gas facilities using a cooperative game approach," *IEEE Transactions on Sustainable Energy*, vol. 11, no. 4, pp. 2545-2555, Oct. 2020.

[20] J. Li, Q. Ai, and S. Yin, "Coordinated bidding and trading strategy for wind power and thermostatic load in a novel market framework," *IET Renewable Power Generation*, vol. 16, no. 5, pp. 1027-1045, Apr. 2022.

[21] A. Jamali, J. Aghaei, M. Esmaili *et al*., "Self-scheduling approach to coordinating wind power producers with energy storage and demand response," *IEEE Transactions on Sustainable Energy*, vol. 11, no. 3, pp. 1210-1219, Jul. 2020.

[22] Jiangsu Development and Reform Commission. (2023, Nov.). Implementation plan of new power system in coastal areas of Jiangsu. [Online]. Available: https://fzggw. jiangsu. gov. cn/art/2023/11/2/art_283_11059865.html

[23] Inner Mongolia Autonomous Region Energy Bureau. (2023, Nov.). Implementation rules of the wind-solar hydrogen production integration project in Inner Mongolia Autonomous Region. [Online]. Available: https://nyj.nmg.gov.cn/zwgk/zfxxgkzl/fdzdgknr/xzgfxwj/202311/t20231117_2412599.html

[24] Eastern Regulatory Bureau of the National Energy Administration. (2022, May). Implementation rules for the management of grid-connected operations in the East China region (draft for soliciting opinions). [Online]. Available: https://hdj. nea. gov. cn/dtyw/tzgg/202402/t20240209_247487.html

[25] T. Meng. (2024, May). Parameters and supplementary formulas in the simulation. [Online]. Available: https://github. com/KatherineMth/For-MPCE_2024/tree/main

[26] EirGrid Group. (2020, Oct.). Northern Ireland wind generation. [Online]. Available: https://www. eirgrid. ie/grid/real-time-system-information

[27] X. Ma, Y. Sun, and H. Fang, "Scenario generation of wind power based on statistical uncertainty and variability," *IEEE Transactions on Sustainable Energy*, vol. 4, no. 4, pp. 894-904, Oct. 2013.

[28] M. Song, W. Sun, M. Shahidehpour *et al*., "Multi-time scale coordinated control and scheduling of inverter-based TCLs with variable wind generation," *IEEE Transactions on Sustainable Energy*, vol. 12, no. 1, pp. 46-57, Jan. 2021.

Tianhui Meng received the B.S. and M.S. degrees in electrical engineering from Harbin Institute of Technology, Harbin, China, in 2016 and 2019, respectively. She is currently working toward the Ph.D. degree in the School of Electrical Engineering and Automation, Harbin Institute of Technology. Her research interests include renewable energy and optimal dispatch of power system.

Jilai Yu received the B.S. and M.S. degrees from Harbin Institute of Technology, Harbin, China, in 1988 and 1990, respectively, and the Ph.D. degree from North China Institute of Electric Power, Baoding, China, in 1992. As a Postdoctoral Researcher, he joined the School of Electrical Engineering, Harbin Institute of Technology, in 1992. He was an Associate Professor in the School of Electrical Engineering, Harbin Institute of Technology, in 1994. He has been a Professor in the School of Electrical Engineering, Harbin Institute of Technology, since 1998. His current research interests include power system analysis and control, optimal dispatch of power system, green power, and smart grid.